Msx2 is an immediate downstream effector of *Pax3* in the development of the murine cardiac neural crest

Stanford J. Kwang[1,*], Sean M. Brugger[2,*], Arthur Lazik[2,*], Amy E. Merrill[2], Lan-Ying Wu[2], Yi-Hsin Liu[1], Mamoru Ishii[2], Frank O. Sangiorgi[1], Michael Rauchman[3], Henry M. Sucov[2], Richard L. Maas[4] and Robert E. Maxson, Jr[2,†]

[1]Center for Craniofacial Molecular Biology, School of Dentistry, University of Southern California, 1441 Eastlake Avenue, Los Angeles, CA 90089-9176, USA
[2]Department of Biochemistry and Molecular Biology, USC/Norris Comprehensive Cancer Center and Hospital, Keck School of Medicine, University of Southern California, 1441 Eastlake Avenue, Los Angeles, CA 90089-9176, USA
[3]Department of Medicine, Renal Division, School of Medicine, Washington University, St Louis, MO 63110, USA
[4]Genetics Division, Department of Medicine, Brigham and Women's Hospital and Harvard, Medical School, Harvard University, Boston, MA 02115, USA
*These authors contributed equally to the experimental work
†Author for correspondence (e-mail: maxson@hsc.usc.edu)

SUMMARY

The neural crest plays a crucial part in cardiac development. Cells of the cardiac subpopulation of cranial neural crest migrate from the hindbrain into the outflow tract of the heart where they contribute to the septum that divides the pulmonary and aortic channels. In *Splotch* mutant mice, which lack a functional *Pax3* gene, migration of cardiac neural crest is deficient and aorticopulmonary septation does not occur. Downstream genes through which *Pax3* regulates cardiac neural crest development are unknown. Here, using a combination of genetic and molecular approaches, we show that the deficiency of cardiac neural crest development in the *Splotch* mutant is caused by upregulation of *Msx2*, a homeobox gene with a well-documented role as a regulator of BMP signaling. We provide evidence, moreover, that Pax3 represses *Msx2* expression via a direct effect on a conserved Pax3 binding site in the *Msx2* promoter. These results establish *Msx2* as an effector of *Pax3* in cardiac neural crest development.

Key words: Cardiac neural crest, Knockout, Mouse, *Msx1*, *Msx2*, *Pax3*, *Splotch*

INTRODUCTION

The neural crest, a migratory cell population originating in the dorsal neural tube, is required for the development of the mammalian heart. The cardiac subpopulation of the neural crest emerges from rhombomeres 6, 7 and 8 of the postotic neural tube and migrates into branchial arches 3, 4 and 6 (Miyagawa-Tomita et al., 1991). Some cells continue migrating into the cephalic region of the heart tube, or outflow tract. There they coalesce into ridges of connective tissue that grow together and ultimately fuse, forming the septum between the aortic and pulmonary channels. Deficiencies of cardiac neural crest development result in a failure of outflow tract septation and defective remodeling of the aortic arch arteries (Creazzo et al., 1998).

The mouse mutant *Splotch* provides an entrée into the molecular circuitry regulating neural crest development. In the homozygous state, the *Splotch* mutation results in several anomalies of neural crest that affect development of melanocytes, dorsal root ganglia, sympathetic ganglia, thymus, thyroid and the outflow septum of the heart (Auerbach, 1954;

Conway et al., 1997b; Conway et al., 1997c; Epstein et al., 2000; Franz, 1989). Defects of neural tube closure and limb musculature development also occur. Several alleles of *Splotch* are known; these cause a spectrum of defects generally similar to those seen in the original *Splotch* mutant, but of varying severity (Dicke, 1964). The outflow tract anomaly of *Splotch* results from a deficiency in the migration of cardiac neural crest cells: *Splotch* cardiac neural crest cells initiate migration but do not reach the branchial arches or the outflow tract in sufficient numbers for aortic arch remodeling or outflow tract septation to occur (Conway et al., 1997b; Epstein et al., 2000; Serbedzija and McMahon, 1997). Deficiencies in myocardial function further compromise cardiac function (Conway et al., 1997a; Li et al., 1999), such that homozygous *Splotch* mutants die in utero at approximately E13.5 and exhibit signs of cardiac insufficiency (Conway et al., 1997c). This myocardial defect is probably an indirect consequence of reduced numbers of migrating crest cells, because neural crest does not contribute to the myocardium (Jiang et al., 2000).

The *Splotch* phenotype is caused by a loss-of-function mutation in *Pax3* (Epstein et al., 1993; Goulding et al., 1993),

one of nine mammalian Pax genes (Stuart et al., 1994; Walther and Gruss, 1991). In humans, loss-of-function mutations in *PAX3* cause Waardenburg syndrome type I and III (Stuart et al., 1994; Machado et al., 2001) in which inactivation of a single *PAX3* allele produces defects stemming from abnormal neural crest development, including sensorineural deafness, pigmentation anomalies, and abnormal skeletal and neurological features (Asher et al., 1996). Cardiac defects have also been reported in children bearing mutations in *PAX3* (Banerjee, 1986; Mathieu et al., 1990). Within the tissues that form the heart, *Pax3* expression is detectable only in cardiac neural crest cells and only during the early phases of their migration, consistent with findings that the *Splotch* mutation acts early in cardiac neural crest development (Conway et al., 2000; Epstein et al., 2000). The *Splotch* cardiac phenotype can be rescued by transgenic expression of *Pax3* under the control of a region of the *Pax3* promoter that expresses in the neural tube and neural crest, suggesting that the defect in neural crest development is cell autonomous (Li et al., 1999).

Little is known about the downstream targets of *Pax3* in cardiac neural crest. Transcripts encoding the proteoglycan versican are upregulated in mesenchyme adjacent to the neural tube of *Splotch* mutant embryos, suggesting a role for this protein in crest migration (Henderson et al., 1997). In other tissues, genes that are potentially downstream of *Pax3* include the gene for receptor tyrosine kinase, *Met*, which is required for the migration of limb muscle precursor cells (Epstein et al., 1996), *Mitf*, a transcription factor associated with Waardenburg syndrome type II (Tassabehji et al., 1994; Watanabe et al., 1998), *Ret*, a tyrosine kinase receptor which is the most often mutated in Hirschsprung disease (Edery et al., 1994; Lang et al., 2000; Romeo et al., 1994), and *Tyrp1*, a tyrosinase-related protein involved in the genesis of pigmentation (Galibert et al., 1999).

We have focused on the potential role of *Msx2* as a *Pax3* effector. *Msx* genes encode homeodomain-containing transcription factors related to the *msh* gene of *Drosophila* (Holland, 1991; Bell et al., 1992). Vertebrates possess three Msx-related genes, *Msx1*, *Msx2* and *Msx3* (Davidson, 1995). *Msx3* is expressed exclusively in the neural tube (Shimeld et al., 1996; Wang et al., 1996). *Msx1* and *Msx2* are expressed in complex and dynamic patterns in a variety of tissues and organs, including the dorsal neural tube and neural crest, where *Pax3* also is expressed (Mansouri et al., 2001; Wang et al., 1996). Targeted inactivation of *Msx1* reveals a role in the development of the molar tooth and palate (Satokata and Maas, 1994). Inactivation of *Msx2* causes defects in calvarial bones, skin and mammary glands. Though not characterized in detail, *Msx1*/*Msx2* double homozygous mutants die in utero at approximately E16, with profound defects in cranial neural crest development (Satokata et al., 2000).

The overlap in the expression domains of *Pax3*, *Msx1* and *Msx2*, together with the involvement of each in neural crest development, prompted us to ask whether these genes interact functionally. Consistent with such a possibility, we found that loss of *Msx2* function rescues the cardiac defect of *Splotch* mutant embryos, as well as defects in the dorsal root ganglia, thymus and thyroid. Both the endogenous *Msx2* gene and transgenes comprising fragments of the *Msx2* promoter fused to *lacZ* were upregulated in the dorsal postotic hindbrain of *Splotch* homozygous mutants, suggesting that *Msx2* is

negatively regulated by *Pax3*. Mutation of a Pax3-binding site within the *Msx2* promoter increased *Msx2* transgene expression in the hindbrain, which reproduced *Msx2* expression in the *Splotch* mutant and provided evidence that *Pax3* is a direct transcriptional repressor of *Msx2*.

MATERIALS AND METHODS

Mouse strains, transgenes and the production of transgenic mice

Splotch, wild-type C57BL/6J and BALB/cJ mice were obtained from the Jackson Laboratory (stocks 000311, 000664 and 000651, respectively). The *Msx1* and *Msx2* knockouts (Satokata and Maas, 1994; Satokata et al., 2000) were produced from ES cells derived from strain 129/SvJ. Germline chimeras were crossed initially into BALB/cJ and then into C57BL/6J for five to six generations. Wild-type 129/SvJ mice were obtained from Dr Peter Laird (USC Medical School). *Δ1Msx2-lacZ* and *Δ2Msx2-lacZ* transgenic mice have been described previously (Liu et al., 1994).

The *Δ3Msx2-hsplacZ* construct contained an 1815 bp Hind*III*-Not*I* fragment located between –5018 and –3203 bp upstream of the *Msx2* translation start site (Liu et al., 1994). This fragment was blunt-ended at Not*I* and cloned into a Hind*III* site and a Sma*I* site immediately upstream of the *hsp68-lacZ*-SV40 cassette (Kothary et al., 1989). The *Δ4Msx2-hsplacZ* construct contained a 560 bp PCR fragment located between –3862 and –3303. The PCR primers introduced an Apa*I* site at the 5′ end a Xho*I* site at the 3′ end. This fragment was cloned into Apa*I*-Xho*I* sites immediately upstream of the *hsp68-lacZ*-SV40 cassette (Kothary et al., 1989).

To generate the Pax site 1 mutant, we used the QuikChange site-directed mutagenesis kit (Stratagene). PCR primers were designed to introduce point mutations in Pax site 1, in the context of the 560 bp promoter fragment *Δ4Msx2-hsplacZ*, as indicated in Fig. 5A, and verified by sequencing. The *Δ4Msx2-hsplacZ* Pax site 1M vector was generated in the same way as described above for the wild-type congener. Transgenic mouse embryos were produced as described previously (Liu et al., 1994).

Histology, in situ hybridization and β-galactosidase detection

Embryos were fixed in 4% paraformaldehyde for 0.5-24 hours, depending on the size of the embryo. They were embedded either in paraffin (for standard histology) or in Historesin after β-gal staining (Lazik et al., 1996). Paraffin-embedded sections were cut at 6 μm, Historesin-embedded sections cut at 4 μm. Hematoxylin and Eosin staining was carried out for histology.

Whole-mount in situ hybridization was performed essentially as described elsewhere (Hogan, 1994). *Msx2* sense and antisense probes were generated by transcription with T3 and T7 RNA polymerase, respectively, and labeled with digoxigenin-labeled UTP. The Pax3 probe, a kind gift from Martyn Goulding, was derived from a 530 bp Hind*III*-Pst*I* fragment of the murine *Pax3* cDNA (Goulding et al., 1991). After whole-mount in situ hybridization, frozen sections (30 μm) were prepared and photographed under Nomarski optics. Photographs were digitized and the images processed in Adobe PhotoShop.

Genotyping and statistical analysis of genetic crosses

DNA was prepared from mouse tails as described (Hogan, 1994). *Splotch* and *Msx2* knockout mutants, and *Msx2-lacZ* transgenes (Liu et al., 1994) genotypes were determined by PCR. Distinguishing the *Splotch* and wild-type *Pax3* alleles required two reactions, one with the UM and CD primers and the other with the UW and CD primers. PCR was performed for 35 cycles with an annealing temperature of 55°C and an expected product of 158 bp. Oligonucleotide primer

sequences for *Pax3* were as follows: wild-type forward (UW), 5′-GTGTGCGCTCCTCTTTTCTCCAG-3′; *Splotch* forward (UM), 5′-CGTGTGCGCTCCTCTTTCGTGTG-3′; and reverse (CD), 5′-CTC-GCTCACTCAGGATGCCATC-3′. Genotyping of *Msx2* knockout mice was performed as previously described (Satokata et al., 2000).

Confidence intervals for *Msx1-Pax3* and *Msx2-Pax3* interactions were computed using the method of Louis (Louis, 1981), which allows calculation of a one-sided confidence interval for a binomial parameter after observing no successes.

Electrophoretic mobility shift assay (EMSA)

Oligonucleotides containing Pax site 1 are as follows: Pax site 1 upper (5′-GCCGAAGTCACACAGCGAATG-3′), Pax site1 lower (5′-TGG-ACATTCGCTGTGTGACTT-3′).

Oligonucleotides containing the high affinity Pax3 site Nf3′ (Epstein et al., 1995): Nf3′ upper (5′-CTAGTGTGTGTGTCACGCT-TATTTTCCTGTACTTATTG-3′), Nf3′ lower (5′-CTAGCAATAA-GTACAGGAAAATAAGCGTGACA-3′).

Oligonucleotides containing a mutant Pax site1 are as follows: 1M upper (5′-GCCGAAGGATATCGTGAAATG-3′), 1M lower (5′-TGG-ACATTTCACGATATCCTT-3′).

Upper and lower strands were annealed, 3′ filled in with ^{32}P-dCTP and Klenow fragment, and purified on Sephadex G-25 columns. Pax3 protein was generated by coupled transcription/translation using the Promega T7 TnT kit. Binding reactions contained 10,000 cpm of oligonucleotide probe, reaction buffer (10 mM Tris-HCl pH7.5, 50 mM NaCl, 7.5 mM MgCl$_2$, 1 mM EDTA, 0.1% NP-40, 5 mM DTT, 5% sucrose, 5% glycerol), 0.5 μg poly d(I-C), and 0.5, 1, 2 or 3 μl lysate in a 15 μl volume. Bovine serum albumin (BSA) was used to equalize the protein concentrations in different reactions. Reactions were carried out at 4°C for 30 minutes, then run on 6% acrylamide gels in Tris-glycine buffer. Gels were dried and autoradiographed.
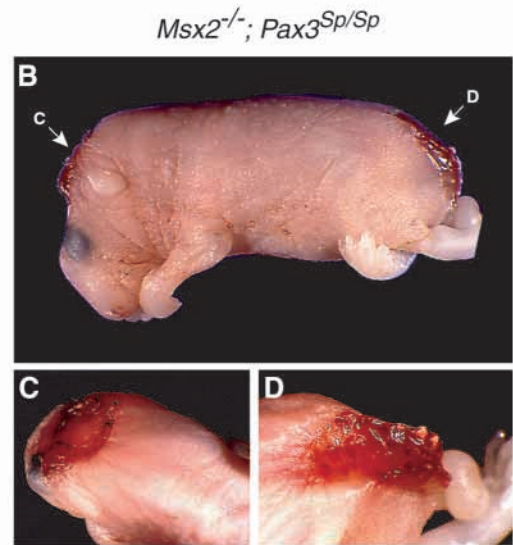
RESULTS

Suppression of embryonic lethality of the homozygous *Splotch* mutation by a targeted mutation in *Msx2* but not in *Msx1*

To investigate the relationship between *Pax3*, *Msx1* and *Msx2*, we intercrossed *Splotch* mutant mice with *Msx1* and *Msx2* knockout mice. Extensive studies conducted on the *Splotch* mutant have shown that virtually 100% of $Pax3^{Sp/Sp}$ animals die in utero at approximately E13.5 of heart failure (Auerbach, 1954; Li et al., 1999). Nearly all such $Pax3^{Sp/Sp}$ animals exhibit spina bifida, which can occur with or without exencephaly (Auerbach, 1954). $Msx1^{-/-}$ animals exhibit cleft palate and tooth defects but survive to term (Satokata and Maas, 1994). $Msx2^{-/-}$ animals have defects in craniofacial structures, skin and mammary gland, but are viable and able to reproduce (Satokata et al., 2000). Neither *Msx1* nor *Msx2* mutant animals have detectable anomalies in the cardiac outflow tract or neural tube (S. K. and R. M., unpublished observations).

Double heterozygous mutant combinations ($Msx1^{+/-}$; $Pax3^{Sp/+}$ and $Msx2^{+/-}$; $Pax3^{Sp/+}$) did not exhibit changes in any *Splotch* mutant phenotypes (not shown). However, intercrosses of $Msx2^{-/-}$; $Pax3^{Sp/+}$ mice revealed a strong and unexpected genetic interaction. Whereas control intercrosses of $Pax3^{Sp/+}$ mice yielded no newborn mice with the $Pax3^{Sp/Sp}$ genotype (0/78), $Msx2^{-/-}$; $Pax3^{Sp/+}$ intercrosses produced a significant fraction of newborns (17/77; 22%) that were homozygous for the *Splotch* mutation (Fig. 1A). All of these animals had spina bifida with or without exencephaly, and all died in the neonatal period (Fig. 1B-D). As $Pax3^{Sp/Sp}$ homozygotes have not been

Fig. 1. Targeted inactivation of *Msx2* but not of *Msx1* suppresses the embryonic lethality of the homozygous *Splotch* genotype. Mice with targeted mutations in *Msx1* or *Msx2* were intercrossed with *Splotch* mutant mice as indicated in A. (B) A gross view of a newborn $Msx2^{-/-}$; $Pax3^{Sp/Sp}$ pup. These mice typically had exencephaly (C), spina bifida (D) and craniofacial abnormalities including a foreshortened snout.

shown to live beyond midgestation, the expected incidence of neural tube defects in term pups generated by crossing *Splotch* heterozygotes is zero. These results suggest that the genetic combination that includes the *Splotch* mutation and the targeted *Msx2* allele enables $Pax3^{Sp/Sp}$ embryos to survive to term.

In contrast to these results, the cross $Msx1^{+/-}$; $Pax3^{+/-} \times Msx1^{+/-}$; $Pax3^{+/-}$ produced no $Pax3^{-/-}$ animals at the newborn stage (0/45) (Fig. 1A). This outcome was significantly different ($P<0.05$) from the expected result if the $Msx1^{-/-}$ or $Msx1^{+/-}$ genotypes could rescue $Pax3^{Sp/Sp}$ embryos to viability. The rescue of $Pax3^{Sp/Sp}$ embryos was therefore correlated specifically with the *Msx2* knockout allele.

We next sought to exclude the possibility that a strain background effect was responsible for the apparent rescue of *Splotch* mutant embryos by the *Msx2* knockout. In the crosses described above, the *Splotch* mutant was in a C57BL/6J background; the *Msx1* and *Msx2* knockouts were in a largely C57BL/6J background (5-6 generations), but were initially in a mixed BALB/cJ and 129/SvJ background (Satokata et al., 2000). Arguing against a strain effect was, first, the fact that *Msx1* mutant mice did not rescue, yet had the same background composition as the *Msx2* mutant mice. Second, there was a tight correlation between the rescue phenotype and the *Msx2* genotype: we did not see any rescued animals that did not carry

the targeted *Msx2* allele. A third argument came from the results of test crosses in which we examined the effect of the BALB/cJ and 129/SvJ backgrounds on the viability of *Pax3^{Sp/Sp}* embryos. We produced *Pax3^{Sp/+}* in mixed C57BL/6J/BALB/cJ and C57BL/6J/129/SvJ backgrounds. We then carried out inter se matings between *Pax3^{Sp/+}* C57BL/6J/BALB/cJ and between *Pax3^{Sp/+}* C57BL/6J/129/SvJ

individuals, and examined the progeny for term *Pax3^{Sp/Sp}* animals. Of 64 newborns in the 129SvJ background, and 85 in the BALB/cJ background, none had neural tube defects and none was *Pax3^{Sp/Sp}*. These data show clearly that neither the 129SvJ nor the BALB/cJ background per se had a detectable effect on the frequency of viable *Pax3^{Sp/Sp}* at the newborn stage ($P<0.001$). We conclude that reduced *Msx2* gene function
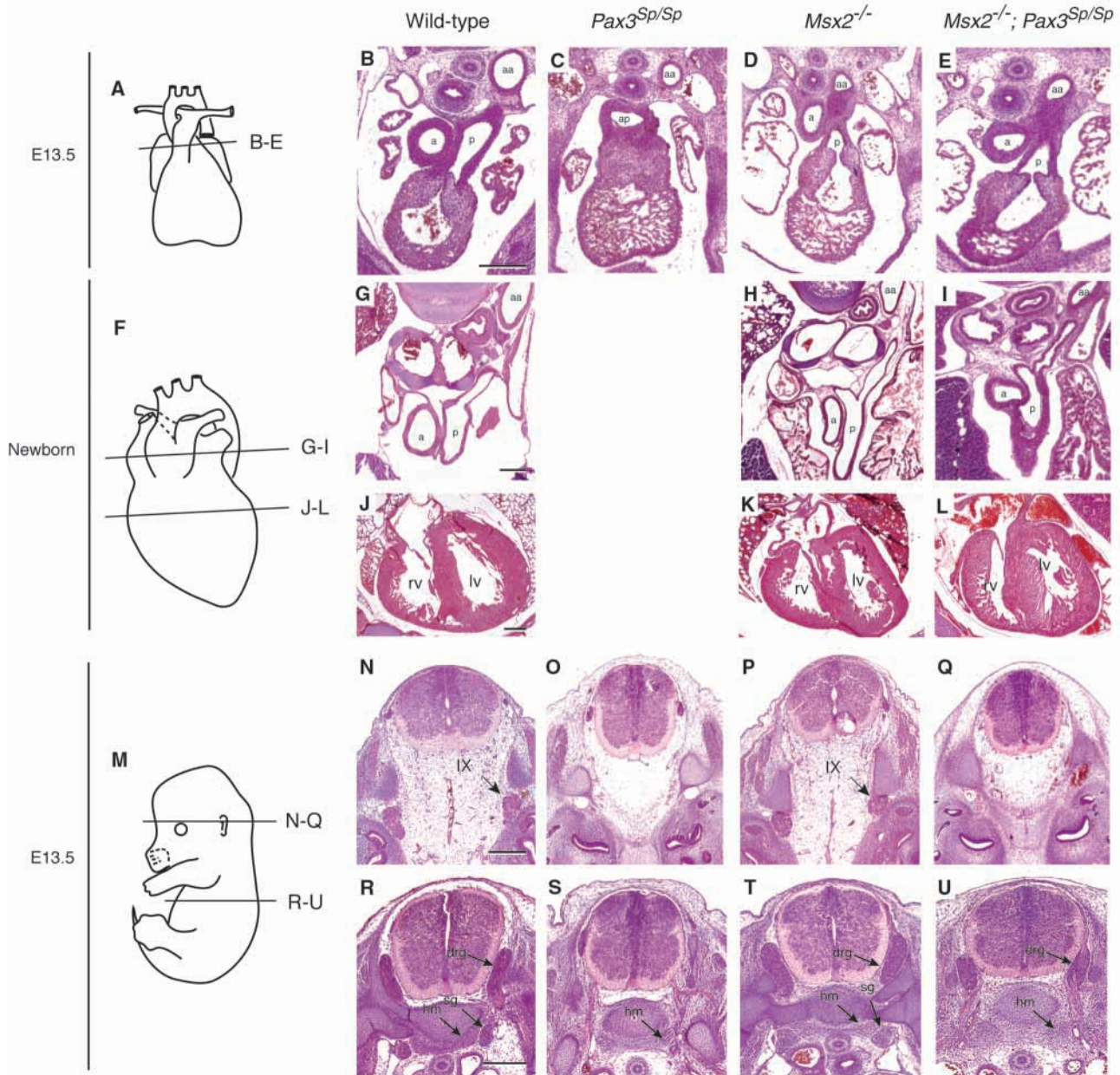
Fig. 2. Targeted inactivation of *Msx2* selectively rescues derivatives of the cardiac neural crest in *Splotch* mutant mice. We show a histological analysis of the influence of a targeted mutation in *Msx2* on neural crest derivatives affected by the *Splotch* mutation. These included the cardiac outflow septum (A-I), the glossopharyngeal (IXth) ganglion (N-Q), dorsal root ganglia and sympathetic ganglia (R-U). The myocardium (J-L), though not derived from neural crest, is known to be affected by the *Splotch* mutation (Li et al., 1999). Note the lack of septation of the aortic and pulmonary channels in the *Pax3^{Sp/Sp}* embryo (C) but normal septation in the *Msx2^{-/-}*; *Pax3^{Sp/Sp}* embryo (E). Note normal morphology of a *Msx2^{-/-}*; *Pax3^{Sp/Sp}* at the newborn stage, both at level of outflow vessels (I) and myocardium (L) compared with wild-type (G,J) and *Msx2^{-/-}* (H,K) animals. Both the glossopharyngeal ganglion and the thoracic sympathetic ganglion are absent in *Pax3^{Sp/Sp}* embryos (O,S). In contrast to the cardiac outflow septum, neither is rescued in *Msx2^{-/-}*; *Pax3^{Sp/Sp}* embryos (Q,U). The dorsal root ganglia, also reduced or absent in *Pax3^{Sp/Sp}* (S), are partially rescued in *Msx2^{-/-}*; *Pax3^{Sp/Sp}* (U) embryos. IX, glossopharyngeal ganglion; a, aorta; aa, arch of aorta at site of entrance of ductus arteriosus; ap, aorticopulmonary trunk; drg, dorsal root ganglion; hm, hypaxial muscle; lv, left ventricle; p, pulmonary trunk; rv, right ventricle; sg, sympathetic ganglion. Scale bar: 500 μm.

specifically rescued *Pax3$^{Sp/Sp}$* embryos to viability at the newborn stage.

Loss of *Msx2* function rescues a subset of neural crest defects in *Pax3$^{Sp/Sp}$* embryos

To determine whether the *Msx2$^{-/-}$* genotype rescued the cardiac neural crest-related phenotypes of *Splotch* homozygous mutants, we compared the morphologies of wild-type, *Msx2$^{-/-}$*, *Pax3$^{Sp/Sp}$* and *Msx2$^{-/-}$*; *Pax3$^{Sp/Sp}$* hearts at E13.5 (Fig. 2B-E) and at newborn (Fig. 2G-L) stages. Analysis of serial transverse sections at E13.5 showed normal outflow tract and aortic arch anatomy in wild-type and *Msx2* knockout embryos (Fig. 2B,D). As expected, *Pax3$^{Sp/Sp}$* embryos (5/7) exhibited either persistent truncus arteriosus, defective remodeling of aortic arch arteries, or both, consistent with an effect on cardiac neural crest development (Fig. 2C). By contrast, all *Msx2$^{-/-}$*; *Pax3$^{Sp/Sp}$* hearts examined (3/3) had normal outflow tract and aortic arch development (Fig. 2E). At the newborn stage, hearts of *Msx2$^{-/-}$*; *Pax3$^{Sp/Sp}$* newborns were grossly normal, with both the ascending aorta and pulmonary artery clearly visible (data not shown). Transverse sections confirmed that the aorta and pulmonary artery were distinct and that there were no aortic arch anomalies (5/5) (Fig. 2I). Sections at the level of the ventricles revealed that the myocardia of the double mutant embryos were indistinguishable from those of wild-type and *Msx2$^{-/-}$* embryos (5/5) (Fig. 2J-L). Thus the *Msx2$^{-/-}$* genotype rescued not only the embryonic lethality of the homozygous *Splotch* mutation, but also the developmental anomalies of the neural crest-derived and neural crest-dependent structures of the *Splotch* mutant heart.

We next asked whether other neural crest-derived structures affected by the *Splotch* mutation were rescued. In *Pax3$^{Sp/Sp}$* embryos, as previously described (Auerbach, 1954; Li et al., 1999), the glossopharyngeal ganglion of the IXth cranial nerve and the sympathetic ganglia were completely absent (Fig. 2O,S; Table 1). The dorsal root ganglia were absent or substantially reduced. The thyroid was reduced in size (data not shown), and the thymus, though visible, failed to undergo migration (data not shown). Analysis of serial transverse sections showed that in *Msx2$^{-/-}$*; *Pax3$^{Sp/Sp}$* double mutant embryos, the sympathetic ganglia were absent at all axial levels (Fig. 2U). Similarly, the glossopharyngeal ganglion, which is derived from r6 (Manzanares et al., 2000), was not rescued by the *Msx2$^{-/-}$* genotype (Fig. 2P-Q). The dorsal root ganglia were visible in double mutant embryos but were reduced in size compared with wild-type or *Msx2$^{-/-}$* embryos (Fig. 2R-U). This

partial rescue of the dorsal root ganglia occurred to an equal extent along the rostrocaudal axis (data not shown). Both the thymus and thyroid were normal (data not shown). The *Msx2$^{-/-}$* genotype thus had a differential effect on different neural crest-derived structures, ranging from a complete rescue of the cardiac outflow septum to no effect on the glossopharyngeal ganglion. We conclude that the functional relationship between *Pax3* and *Msx2* differs in individual subpopulations of neural crest.

We did not observe any modification of non-neural crest phenotypes in *Pax3-Msx2* double mutants compared with *Splotch* mutants. Two classes of neural tube defects were found in the double homozygous (*Msx2$^{-/-}$*; *Pax3$^{Sp/Sp}$*) pups that escaped midgestation death and survived to term: spina bifida alone (64%), and exencephaly and spina bifida together (36%). Analyses of *Pax3$^{Sp/Sp}$* animals in utero yielded similar percentages (data not shown). The diaphragm muscle of *Msx2$^{-/-}$*; *Pax3$^{Sp/Sp}$* double mutant pups was absent, and these mice did not breathe at birth (data not shown), demonstrating that the *Msx2$^{-/-}$* genotype did not rescue muscle development in *Splotch*. The effect of the *Msx2$^{-/-}$* genotype on *Splotch* mutants was therefore specific to a limited number of neural crest-derived structures.

Upregulation of *Msx2* in the postotic hindbrain of *Splotch* mutant embryos

The simplest model to explain the genetic interaction between *Msx2* and *Pax3* in cardiac development is that *Pax3* negatively regulates *Msx2* gene activity in the cardiac neural crest or in a tissue that influences the development of the cardiac neural crest. The *Splotch* cardiac phenotype can be rescued by expression of *Pax3* driven by a segment of the *Pax3* promoter that directs expression to the neural tube and neural crest (Li et al., 1999); thus, we expected the interaction between *Msx2* and *Pax3* would occur in one or both of these tissues. As *Pax3* is downregulated soon after cardiac neural crest cells emigrate from the postotic hindbrain at E9-10 (Conway et al., 1997c; Epstein et al., 2000), we also predicted that any functionally important change in *Msx2* expression would occur in the dorsal neural tube or in the neural crest during the early phases of its migration. Accordingly, we tested the effect of the *Splotch* mutation on *Msx2* expression in the hindbrain and neural crest at E9.5.

Whole-mount in situ hybridization experiments on wild-type embryos showed that *Msx2* was expressed strongly in r5, and lower at levels caudally (Fig. 3B,E). *Pax3*, by contrast, was expressed at relatively lower levels in the otic region (r4 and r5) but at higher levels caudally (Fig. 3A,D). In *Splotch* mutant embryos, there was an increase in the intensity of the *Msx2* hybridization signal in the postotic hindbrain relative to the otic region (Fig. 3C,F).

Transverse sections of whole-mount preparations showed that at the level of the otic vesicle (r5), *Msx2* was expressed in the dorsal neural tube while *Pax3* was expressed more ventrally and laterally (Fig. 3G,H). In the postotic neural tube (r6-8), *Msx2* was expressed in a medial to lateral gradient, with the highest levels medially (Fig. 3K). *Msx2* was expressed at a relatively low level in the mid-dorsal region of the neural tube (Fig. 3K), while *Pax3* transcripts were present throughout the dorsal neural tube (Fig. 3J). In *Splotch* mutant embryos, *Msx2* expression expanded, occupying a greater proportion of the *Pax3* domain than in wild-type embryos. This was particularly

Table 1. Influence of *Msx2$^{-/-}$* genotype on *Pax3$^{Sp/Sp}$* neural crest phenotypes

	Wild-type	*Msx2$^{-/-}$*	*Pax3$^{Sp/Sp}$*	*Pax3$^{Sp/Sp}$*; *Msx2$^{-/-}$*
Cardiac outflow tract	+	+	−	+
Dorsal root ganglia	+	+	−	+/−
Thoracic sympathetic ganglia	+	+	−	−
Thyroid	+	+	−	+
Thymus	+	+	−	+
Glossopharyngeal nerve (IX)	+	+	−	−

The indicated structures were examined histologically (see Fig. 2).
−, a substantial morphological deficiency; +, a wild-type appearance. See text for details.
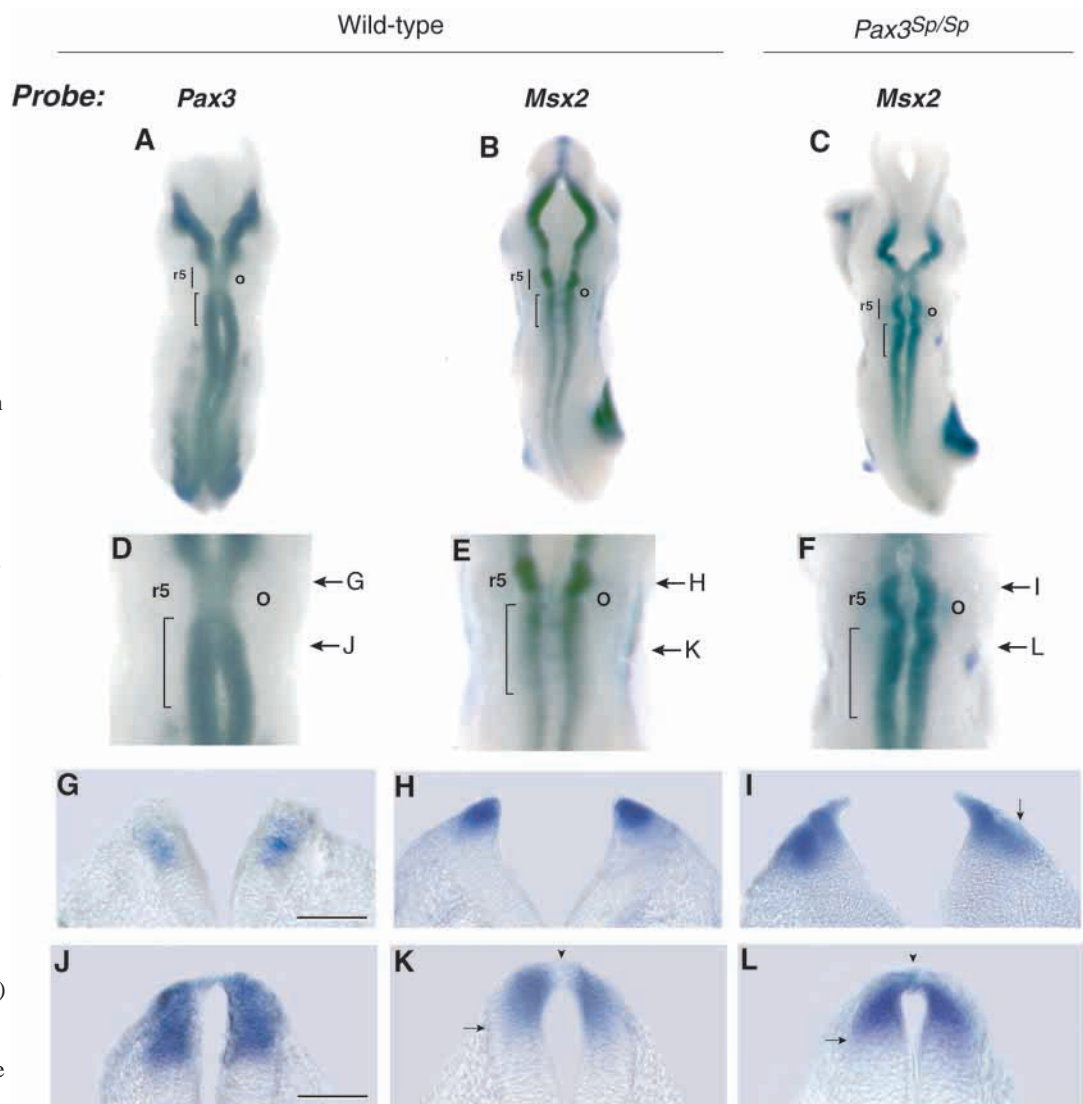
Fig. 3. Altered expression of *Msx2* in *Splotch* mutant embryos. Embryos at E9.5 were allowed to hybridize with digoxygenin-labeled antisense probes against *Pax3* (A,D,G,J) and *Msx2* (B,C,E,F,H,I,K,L). (A,B,D,E,G,H,J,K) Wild-type embryos; (C,F,I,L) *Pax3*^{Sp/Sp} embryos. Brackets indicate the region of the postotic hindbrain from which the cardiac neural crest originates. (D-F) are higher magnification views of hindbrain region of images shown in A-C. (G-L) Cross sections of embryos shown in A-C. Arrows to the right of D-F indicate the levels of the transverse sections. Sense probes did not hybridize detectably (not shown). Note the expansion of *Msx2* expression in dorsal (arrowhead) and lateral (arrow) regions of postotic neural tube of *Pax3*^{Sp/Sp} embryos (L). o, otic vesicle; r5, rhombomere 5. Scale bars: 100 μm.

evident in the postotic hindbrain (r6-8), where *Msx2* expression expanded into the dorsal and lateral regions of the neural tube (Fig. 3L). These data are consistent with the prediction of our genetic experiments that *Pax3* negatively regulates *Msx2* in the postotic hindbrain and neural crest.

A 560 bp segment of the *Msx2* promoter is sufficient for upregulation of *Msx2* transgenes in the postotic hindbrain of *Splotch* mutant embryos

To determine whether the increase in the *Msx2* expression in *Splotch* mutant embryos was caused by an effect on *Msx2* promoter activity, we asked whether transgenes containing regions of the *Msx2* promoter fused to a *lacZ* reporter were upregulated in *Splotch* mutant embryos. We first used two previously characterized transgenic lines (Liu et al., 1994; Liu et al., 1999). One included a 13 kb *Msx2* genomic fragment with a *lacZ* gene inserted near the 5′ end of the first exon (*Δ1Msx2-lacZ*; Fig. 4A), the other a 6.2 kb genomic fragment fused to a *lacZ* reporter (*Δ2Msx2-lacZ*; Fig. 4A). The embryonic expression patterns of several independent *Δ1Msx2-lacZ* and *Δ2Msx2-lacZ* lines have been documented previously (Liu et al., 1994; Liu et al., 1999). Both were found to

recapitulate endogenous *Msx2* expression accurately in a variety of sites in the embryo, including the hindbrain and migratory cardiac neural crest (Liu et al., 1994; Liu et al., 1999; Lazik, 1999).

We crossed the *Δ1Msx2-lacZ* and *Δ2Msx2-lacZ* transgenic mice with *Splotch* mutant mice. Embryos hemizygous for the *Msx2-lacZ* transgenes and homozygous for the *Splotch* mutation were examined at E9.5 for β-galactosidase (β-gal) activity. In whole-mount preparations of E9.5 *Splotch* mutant embryos, both the *Δ1Msx2-lacZ* and *Δ2Msx2-lacZ* transgenes were upregulated in the postotic hindbrain (Fig. 4B,C) similarly to the endogenous *Msx2* gene (Fig. 3F). We prepared both transverse sections and longitudinal sections through the hindbrains of such embryos and examined them under dark field, which affords greater sensitivity than standard bright field imaging (Lazik et al., 1996). Stronger signals are blue, weaker signals pink. Transverse sections through the postotic hindbrain showed an increase in β-gal activity in the dorsal neural tubes of homozygous *Splotch* mutant embryos relative to wild type (Fig. 4D,E). These changes were similar to those of endogenous *Msx2* transcripts (Fig. 3K,L).
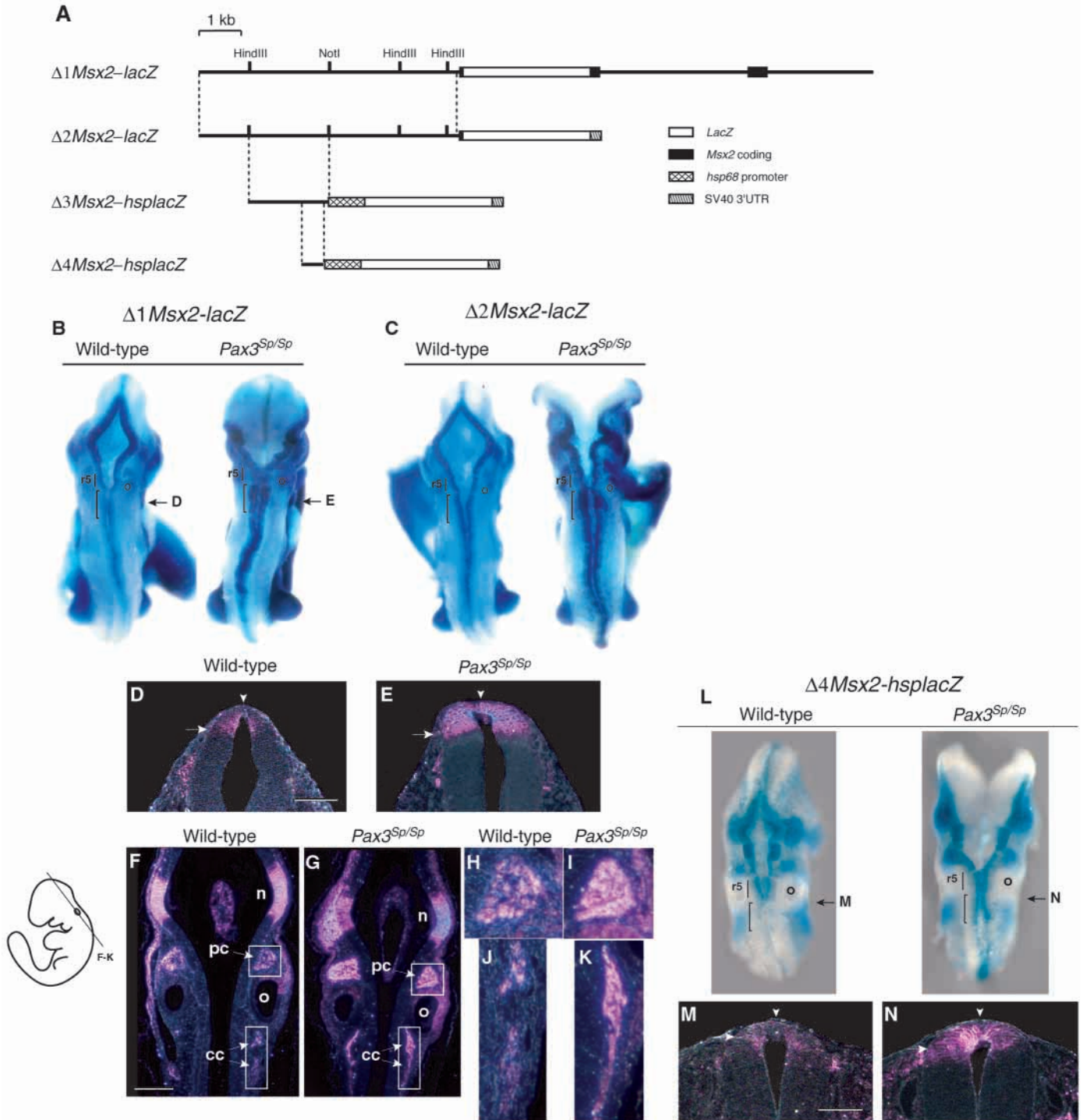
Fig. 4. Transgenic analysis identifies a 560 bp Pax3-responsive region within the *Msx2* promoter. (A) Schematic maps of *Msx2-lacZ* transgene constructs. *Δ1* and *Δ2* contain a *lacZ* gene inserted in the first exon. *Δ3* and *Δ4* comprise the indicated promoter fragments fused to an *hsp68* minimal promoter and *lacZ* reporter. (B-N) Effect of the *Splotch* mutation on transgene expression in E9-9.5 embryos. (B,C,L) Dorsal views of whole-mount preparations. Brackets indicate the approximate location of the cardiac neural crest. Note increased staining in the postotic hindbrain of *Δ1Msx2-lacZ*, *Δ2Msx2-lacZ* and *Δ4Msx2-lacZ* transgenes in *Pax3^{Sp/Sp}* embryos. The embryos in L are at a slightly earlier stage than those in B,C, which accounts for the lower overall level of staining in the hindbrain and neural tube. Embryos in B and L were sectioned in the transverse plane. Shown below the whole mounts are sections (D,E,M,N) at the levels indicated by arrows to the right of whole mounts. β-gal expression is imaged in dark field. Pink indicates a low to moderate signal, blue a more intense signal. Note the expansion of β-gal expression into the dorsal (arrowhead) and lateral (arrow) regions of the neural tube of *Splotch* mutant embryos, mirroring the change in endogenous *Msx2* expression (Fig. 3). (F,G) Longitudinal sections through the hindbrains of E9.5 *Δ1Msx2-lacZ* embryos. (H-K) Higher magnification views of the boxed regions in F,G. Note increased staining in both preotic crest and cardiac crest in *Splotch* embryos compared with wild type. cc, cardiac crest; n, neural fold; o, otic vesicle; pc, preotic crest; r5, rhombomere 5. Scale bars: 100 μm.

In longitudinal sections of *Splotch* mutant embryos, increased β-gal staining was also evident in streams of migratory cranial neural crest (Fig.4F-K). Serial sections revealed that in wild-type embryos, these streams extended from the preotic and postotic hindbrain into the branchial arches and cardiac outflow tract (data not shown). In *Splotch* mutant embryos, the postotic stream of β-gal-positive crest did not extend into the branchial arches and outflow tract, but rather remained in a small cluster adjacent to the dorsal neural tube. Preotic streams of β-gal-positive crest were unaffected in *Splotch* mutant embryos (data not shown). These results are consistent with previous findings that cardiac neural crest cells in *Splotch* mutant embryos exit the neural tube but do not reach the outflow tract in normal numbers (Epstein et al., 2000).

To further localize the *Pax3*-responsive region of the *Msx2* promoter, we surveyed a series of fragments within the 6.2 kb 5′ flanking sequence for their ability to direct reporter gene expression to the hindbrain. A 1.8 kb fragment (*Δ3Msx2-hsplacZ*, Fig. 4A) was found to be sufficient for hindbrain expression (not shown). Further deletion analysis within this fragment identified a 560 bp fragment, designated *Δ4Msx2-hsplacZ* (Fig. 4A), that was expressed in neural tubes of E9.5 embryos in a manner consistent with endogenous expression. We crossed transgenic mice carrying the 560 bp *lacZ* transgene (two independent lines) with *Splotch* mutants and examined transgene expression in the hindbrain. As can be seen in whole-mounts (Fig. 4L), transgene expression was upregulated in the postotic hindbrain of *Splotch* mutants relative to wild-type or heterozygous mutant embryos. Transverse sections immediately caudal to the otic vesicle showed that transgene expression in the neural tube expanded laterally and ventrally (Fig. 4M,N). This upregulation was similar to that of the endogenous *Msx2* gene, as well as the 13 kb and 6.2 kb transgenes. These data show that a 560 bp segment of the *Msx2* promoter is sufficient to respond to *Pax3* inactivation.

A *cis*-regulatory element that binds Pax3 and inhibits *Msx2* transgene expression in the postotic hindbrain

We next asked whether the effect of *Pax3* on *Msx2* transgene expression occurs via a direct interaction with *cis*-regulatory elements in the *Msx2* promoter. A Blast search of the human genome with the *Pax3*-responsive 560 bp *Msx2* promoter segment produced a single hit at the human MSX2 locus 95 kb upstream of the translation start (Fig. 5A). The murine and human sequences exhibited 87% identity over 520 bp. Within this region of identity was a single consensus Pax3 site (Chalepakis and Gruss, 1995; Epstein et al., 1996; Galibert et al., 1999). This site was also similar to a 14 bp region of the tyrosinase-related protein 1 (*Tyrp1*) promoter that binds Pax3 and is required for Pax3-mediated transactivation in co-transfection assays (Fig. 5A) (Galibert et al., 1999).

The similarity of the human and murine *Msx2* sequences, together with our genetic data identifying the 560 fragment as Pax3-responsive, suggested that the conserved Pax3 site might be involved in the upregulation of *Msx2* in *Splotch* mutant embryos. EMSA experiments showed that Pax site 1 was capable of binding recombinant Pax3 protein with an affinity comparable with a known high affinity Pax3 binding site (Fig. 5B) (Epstein et al., 1995). A 6 bp base substitution mutation (Pax site 1M) substantially reduced the ability of the Pax site

Table 2. Effect of Pax site 1 mutation on Δ4*Msx2-hsplacZ* transgene expression

	Expressing F_0/ transgenic F_0	Transgene upregulation in neural tube
Δ4Msx2-hsplacZ	11/13	0/11
Δ4Msx2-hsplacZ (Pax site 1 mutant)	7/10	7/7

Embryos were analyzed for β-gal expression transiently at stages from E9.5 to E11.5. Upregulation of mutant transgenes in the dorsal neural tube was assessed by comparison with the expression of control transgenes (*Δ4Msx2-hsplacZ* and *Δ1Msx2-lacZ*), which were expressed identically in the dorsal neural tube. All staining was performed under the same conditions.

1 probe to bind Pax3 (Fig. 5B). These results show that Pax site 1 is capable of binding Pax3 specifically.

To test whether Pax site 1 has a functional role in the control of *Msx2* transgene expression in the hindbrain, we introduced the 6 bp Pax site 1 mutation (Pax site 1M) into the 560 bp *lacZ* transgene (*Δ4Msx2-hsplacZ Pax site 1M*). We injected this construct into mouse zygotes and analyzed transgenic embryos transiently at E9.5. As is apparent in Fig. 5D, the *Δ4Msx2-hsplacZ* bearing the Pax site 1 mutation exhibited expanded expression in the neural tubes of E9.5 embryos relative to the *Δ4Msx2-hsplacZ* control embryo (Fig. 5C) (Table 2). Transverse sections of E9.5 embryos revealed a lateral and ventral expansion of the β-gal signal (Fig. 5E,F) similar to that observed for the *Δ1Msx2-lacZ* and *Δ4Msx2-hsplacZ* transgenes in the *Splotch* background (Fig. 4E,N). Some β-gal activity was also observed in the ventromedial region of the neural tube, outside the domain of *Pax3* expression (Fig. 5F), suggesting that *trans*-regulatory factors other than *Pax3* may act through Pax site 1 to inhibit the expression of the *Δ4Msx2-hsplacZ* transgene in the ventral neural tube. A 140 bp deletion of the Pax site 1 and surrounding DNA caused a similar upregulation of transgene expression in the postotic neural tube (data not shown), supporting the view that the Pax site 1 mutation inactivates a repressive *cis*-regulatory element. In summary, our results suggest that Pax site 1 functions in the control of *Msx2* expression in the neural tube and neural crest, and that it does so through a direct interaction with Pax3.

DISCUSSION

We provide genetic and molecular evidence in support of a functional interaction between *Pax3* and *Msx2* in mammalian cardiac development. We show that loss of *Pax3* function leads to upregulation of *Msx2* in the neural tube and cardiac neural crest. A genetic manipulation that prevents the upregulation of *Msx2* rescues *Splotch* mutants to viability and also rescues the cardiac morphological defects, providing evidence that increased expression of *Msx2* is causally related to the deficiency in cardiac neural crest development in the *Splotch* mutant mouse. A mutation that interferes with Pax3 binding to a conserved consensus site within the *Msx2* promoter causes an upregulation of *Msx2* transgene expression in the postotic hindbrain similar to that observed for the endogenous *Msx2* and *Msx2* transgenes in *Splotch*. These results suggest that *Pax3* normally acts to suppress *Msx2* function, and furthermore suggest that *Msx2* is a direct transcriptional target of *Pax3*.
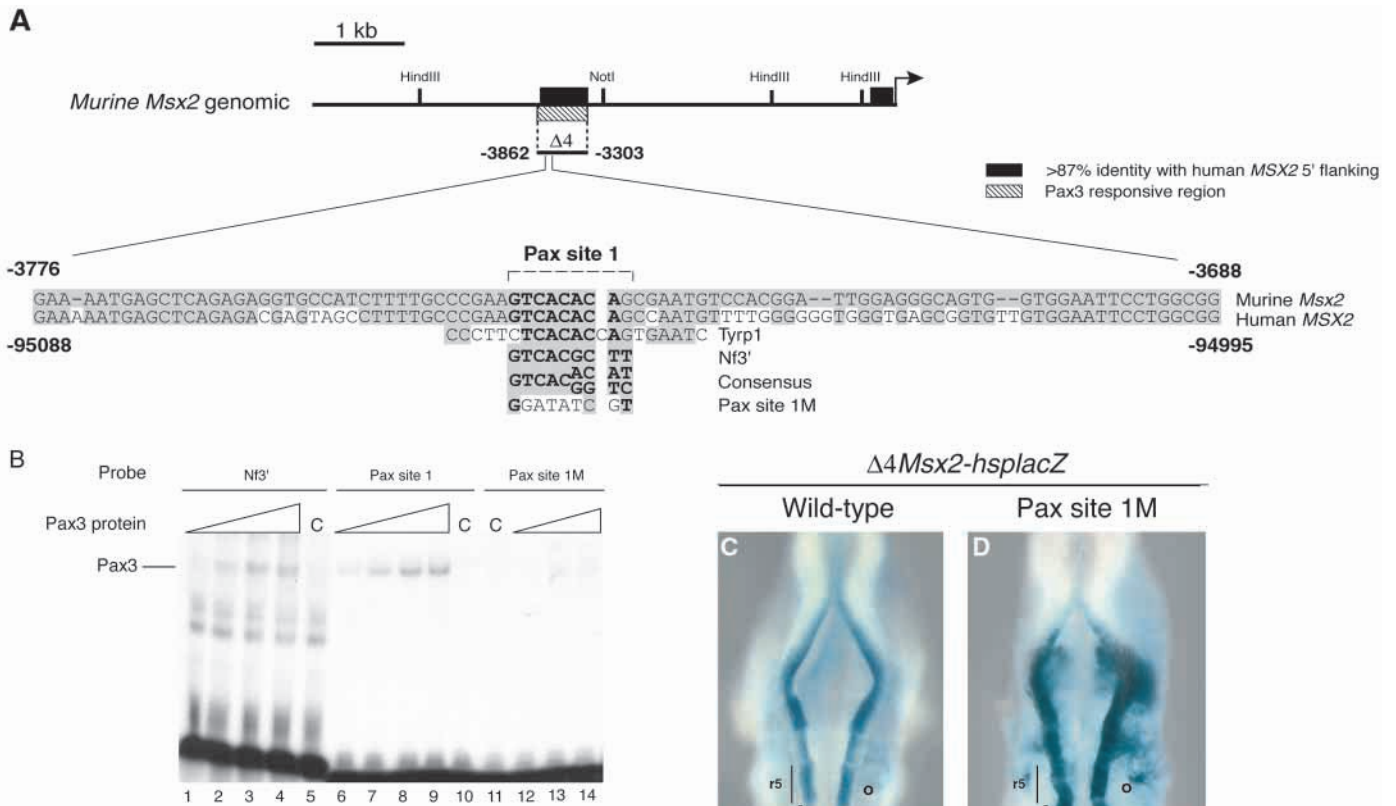
Fig. 5. Mutation of a conserved Pax3-binding site causes upregulation of an *Msx2* transgene in the postotic hindbrain. (A) Alignment of homologous regions of human and murine *Msx2* 5′ flanking sequence. A stretch of 520 bp within the Pax3 responsive region matched closely (87% identity) with a region in the 5′ flanking sequence of the human *MSX2* gene. This stretch included a single, highly conserved Pax3 binding site (Pax site 1). We show the nucleotide sequence of Pax site 1 and surrounding DNA aligned with the human *MSX2* locus. Also shown is a Pax3 site in the *Tyrp1* promoter (Galibert et al., 1999), a high-affinity Pax3-binding site, Nf3′ (Epstein et al., 1995) and the Pax3 consensus (Chalepakis and Gruss, 1995; Epstein et al., 1996). Pax site 1M is a base substitution mutant of Pax site 1. Bold letters show identity with the consensus sequence. (B) Protein titration EMSA analysis of Pax3 binding to Nf3′, Pax site 1 and Pax site 1M. In vitro synthesized Pax3 protein (0.5, 1, 2 and 3 μl) was incubated with radiolabeled Nf3′ (lanes 1-4), Pax site 1 (lanes 6-9) or Pax site 1M (lanes 12-14). Mock transcription-translation lysate (no DNA added) (1 μl) was used as a background control (lanes 5,10,11). Protein-DNA complexes were visualized by autoradiography. (C-F) Effect of Pax site 1 mutation on *Δ4Msx2-hsplacZ* transgene expression. Embryos carrying either the *Δ4* or *Δ4* Pax site 1M transgene were stained at E9.5 for β-gal expression. (C,D) Dorsal views of whole mounts. The region of the neural tube from which the cardiac neural crest originates is indicated by brackets. The position of rhombomere 5 (r5) is shown to the left, the otic vesicle (o) to the right. Note elevated X-gal staining in the postotic neural tube of the Pax site 1 mutant embryo compared with the wild type. (E,F) Sections through the postotic neural tubes (arrows) of the embryos in (C,D). Note ventral and lateral expansion of X-gal stain in mutant (F) relative to wild-type (E) (arrows). Also note ectopic stain in ventromedial neural tube of mutant (F) (arrowhead). Scale bar: 100 μm.

Upregulation of *Msx2* is necessary for the development of the *Splotch* cardiac phenotype

Despite a report suggesting that the ability of neural crest cells to migrate in vitro is impaired by the *Splotch* mutation (Moase and Trasler, 1990), more recent studies have shown that the *Splotch* mutation does not affect migration per se, but rather results in (1) a reduction in the number of cardiac neural crest cells emigrating from the neural tube (Conway et al., 2000); and (2) subtle impairment of the guidance of migrating crest cells such that they do not reach the outflow region in sufficient

numbers to allow normal morphogenesis of the outflow septum or remodeling of the aortic arch arteries (Epstein et al., 2000). Furthermore, these defects are likely to be cell-autonomous, as they can be rescued by expression of wild-type *Pax3* driven by a neural crest- and neural tube-specific region of the *Pax3* promoter (Li et al., 1999).

Our genetic analysis shows that *Msx2* is a part of the regulatory machinery through which *Pax3* controls neural crest development. Whereas homozygous *Splotch* mutants die at E13.5, *Msx2-Pax3* double homozygous mutants survive to the

newborn stage and exhibit normal cardiac outflow and myocardial anatomy. That *Msx2* is upregulated in the hindbrains of *Splotch* mutant embryos, the site of origin of the cardiac neural crest, together with the finding that a genetic manipulation that reduces *Msx2* gene function can rescue the cardiac neural crest defects of *Splotch* suggests that upregulation of *Msx2* is required for the *Splotch* cardiac neural crest defects. The simplest explanation for how a deficiency in *Msx2* can rescue the *Splotch* cardiac neural crest phenotype is that the *Msx2* deficiency restores the ability of cardiac neural crest cells to migrate appropriately to their destinations in the outflow tract. However, other explanations, such as the respecification of other crest populations or a compensatory increase in the proliferative activity of cardiac crest cells, remain possible.

The interaction between *Pax3* and *Msx2* is remarkably cell-type specific. Reduced *Msx2* activity does not rescue the *Splotch* muscle or neural tube defects, nor does it rescue all *Splotch* neural crest defects. While the cardiac neural crest, thymus and thyroid defects are suppressed completely in the *Msx2-Pax3* double mutant, other *Pax3*-related neural crest defects are either partially rescued or unaffected. It is particularly striking that the glossopharyngeal ganglion, which is formed from neural crest originating from r6, within the rostrocaudal domain of the cardiac neural crest (Manzanares et al., 2000), is not rescued. This differential effect of the *Msx2* genotype on different crest populations suggests that the regulatory interaction between *Pax3* and *Msx2* in the cardiac neural crest occurs after the specification of the crest population that gives rise to the outflow septum, thymus and thyroid, and the crest population that gives rise to the cranial and sympathetic ganglia. As *Pax3* is downregulated shortly after crest cells emigrate from the neural tube (Epstein et al., 2000), it is likely that cardiac crest is specified before its migration into the outflow tract.

Nonequivalence of *Msx1* and *Msx2* as modifiers of *Pax3*

Our genetic data show that loss of *Msx1* function does not rescue *Splotch* mutants to viability. Although we have not examined the hearts of *Msx1-Pax3* double mutant embryos, the simplest explanation for this lack of rescue is that the *Msx1* knockout fails to suppress the lethal cardiac defect of *Splotch*. This apparent non-equivalence of *Msx1* and *Msx2* is surprising as analysis of *Msx1-Msx2* double mutant phenotypes suggests that these genes function redundantly in the development of at least some structures derived from the cranial neural crest, including the calvarial bones (Satokata et al., 2000). The inability of the *Msx1* mutation to rescue the *Splotch* mutant is not due simply to non-responsiveness of *Msx1* to regulation by *Pax3*: our in situ hybridization results show that *Msx1* is upregulated in the postotic hindbrain of *Splotch* mutant embryos in a manner similar to *Msx2* (data not shown). The failure of the *Msx1* mutant to rescue is therefore more likely to be related to functional differences between the Msx1 and Msx2 proteins, which have virtually identical homeodomains but distinct N-terminal and C-terminal domains (Bell et al., 1993).

Role of Pax3 in the regulation of *Msx2* transcription

Three lines of evidence support the hypothesis that *Pax3* regulates *Msx2* through a direct effect on its promoter. First, *Msx2 lacZ* transgenes are upregulated in the dorsal neural tube of *Pax3*[Sp/Sp] embryos in a manner similar to the endogenous *Msx2* gene. Second, the 560 bp *Pax3*-responsive region of the *Msx2* promoter includes a 520 bp stretch that is highly conserved (87%) in 5′ flanking DNA of the human *MSX2* gene. Within this stretch is a single conserved Pax3 consensus site that Pax3 binds with high affinity. Third, mutation of this element, designated Pax site 1M, causes upregulation of *Msx2 lacZ* transgene expression in the dorsal neural tube. This upregulation is similar in spatial pattern to that of the *Msx2 lacZ* transgenes in the *Splotch* mutant background. These data strongly suggest that Pax3 regulates *Msx2 lacZ* transgenes through a direct interaction with Pax site 1. Whether Pax site 1 is functional in the context of the endogenous *Msx2* promoter is unclear, though our in situ hybridization data show that in the *Splotch* mutant background, the changes in the pattern of endogenous *Msx2* expression are strikingly similar to those of the *Δ4Msx2-hsplacZ* transgene bearing a mutation in Pax site 1. An analysis of approximately 13 kb of genomic sequence flanking the *Msx2* gene has thus far failed to identify additional elements capable of driving *hsp68-lacZ* expression in the neural tube and neural crest; thus Pax site 1 may be of crucial importance in the context of the endogenous *Msx2* promoter.

The molecular defect in *Splotch* is an A→T transversion in a splice acceptor site, which results in four aberrant transcripts (Epstein et al., 1993). Three of these are predicted to produce truncated proteins; one can direct the synthesis of a near full-length protein that lacks only 45 amino acids encoded by exon 4 (Pax3-Δ exon4). This deleted segment comprises a region of the paired domain and the highly conserved octapeptide motif. The paired domain is required for DNA binding (Machado et al., 2001). The octapeptide motif is involved in dimerization and other protein-protein interactions (Chalepakis et al., 1994; Machado et al., 2001). Although transcripts that lack exon 4 have been detected in *Pax3*[Sp/Sp] embryos, whether they are translated is not known. Our finding that a mutation in Pax site 1 in the *Msx2* promoter results in upregulation of an *Msx2* transgene similar to the upregulation of endogenous *Msx2* in *Pax3*[Sp/S]mutant mice is consistent with the view that the molecular lesion in *Splotch* mutants is either a simple absence of Pax3 protein (owing, for example, to destabilization of the mutant protein), or is a result of a failure of the mutant Pax3 protein to form a functional complex on the target DNA. Despite lacking a portion of the paired domain, the Pax3-Δ exon 4 protein is capable of binding DNA (Chalepakis et al., 1994). That this protein lacks the octapeptide motif suggests that if the Pax3-Δ exon 4 transcript is in fact produced and translated in the cardiac neural crest, then its protein product may fail to recruit a partner required for transcriptional repression. Candidates for such a repressor include Groucho-related and Daxx proteins, both of which can interact with Pax3 through the octapeptide motif (Eberhard et al., 2000; Hollenbach et al., 1999). Daxx requires, in addition to the octapeptide, sequences within the homeodomain for interaction with Pax3 (Hollenbach et al., 1999). It is intriguing that the *Splotch*[2H] mutant, which also exhibits defective outflow tract development (Conway et al., 1997b), has a 32 bp deletion in the homeodomain (Epstein et al., 1993). Thus a common molecular mechanism, which involves an interaction between Pax3 and Daxx or another transcriptional repressor,

may lead to increased *Msx2* expression and consequently to cardiac neural crest defects in both *Splotch* and *Splotch²ᴴ* mutant mice.

Finally, we note that the mutation in Pax site 1 not only causes *Msx2* transgene expression to expand into the *Pax3* expression domain, but also causes a low level of ectopic expression in the ventromedial neural tube, outside the *Pax3* domain. This ectopic expression raises the possibility that proteins in addition to *Pax3* may bind Pax site 1 and repress *Msx2* expression in the ventral neural tube. Candidates for such proteins include Pax6, which, like Pax3, binds Pax site 1 avidly (M. R., unpublished), and is known to be expressed in the ventral neural tube (Gruss and Walther, 1992). Members of the brachyury-related T-box protein family are also candidates. The Tyrp1 regulatory elements MSEu and MSEi contain the sequence TCACAC, which has been shown to bind not only Pax3, but also Tbx2 (Carreira et al., 1998; Galibert et al., 1999). The MSEu and MSEi sites are required for both Pax3 and Tbx2 mediated regulation of Tyrp1 in melanocytes (Galibert et al., 1999).

Msx2, *Pax3* and BMP signaling

That *Msx2* has a well-documented role as a bone morphogenetic protein (BMP) effector (Weinstein and Hemmati-Brivanlou, 1999) raises the question of whether the BMP pathway figures in the *Splotch* neural crest defects and the genetic interaction between *Msx2* and *Pax3*. Misexpression experiments have shown that elevated levels of *Bmp4* can induce apoptosis in neural crest that originates from the preotic and otic hindbrain (r3 and r5) (Graham et al., 1994). Overexpression of *Msx2* alone can cause a similar effect (Takahashi et al., 1998). Although apoptosis has not been reported in neural crest cells in *Splotch* mutants, the possibility that the neural crest defects of *Splotch* are a result of ectopic or upregulated BMP signaling, and that loss of *Msx2* function suppresses these effects by attenuating such signaling, is nevertheless an attractive hypothesis.

It is intriguing that *Msx1*, whose expression is positively regulated by BMP2/4, can inhibit the myogenic activity of *Pax3* (Bendall et al., 1999). This effect, which occurs via a direct protein-protein interaction, antagonizes the stimulation of *MyoD* transcription by Pax3 and consequently antagonizes the terminal differentiation of muscle precursor cells. It is important to point out that this mechanism is fundamentally different from the interaction between *Msx2* and *Pax3* in cardiac crest development on both genetic and molecular levels. In the cardiac crest, *Msx2* is genetically downstream of *Pax3*, not upstream as would be predicted by the *Msx1-Pax3* model. In addition, *Pax3* regulates *Msx2* via an effect on its promoter. Nevertheless, findings that *Msx1* and *Msx2*, both BMP effectors, can influence the activity of *Pax3* in muscle precursors and neural crest respectively, raise the possibility of a general role for Msx genes, *Pax3* and the BMP pathway in the development of migratory mesenchymal cell populations.

REFERENCES

Asher, J. H., Jr, Harrison, R. W., Morell, R., Carey, M. L. and Friedman, T. B. (1996). Effects of Pax3 modifier genes on craniofacial morphology, pigmentation, and viability: a murine model of Waardenburg syndrome variation. *Genomics* **34**, 285-298.

Auerbach, R. (1954). Analysis of the developmental effects of a lethal mutation in the house mouse. *J. Exp. Zool.* **127**, 305-329.

Banerjee, A. K. (1986). Waardenburg's syndrome associated with ostium secundum atrial septal defect. *J. R. Soc. Med.* **79**, 677-678.

Bell, J., Char, B. R. and Maxson, R. (1992). An octamer element is required for the expression of the alpha H2B histone gene during the early development of the sea urchin. *Dev. Biol.* **150**, 363-371.

Bell, J. R., Noveen, A., Liu, Y. H., Ma, L., Dobias, S., Kundu, R., Luo, W., Xia, Y., Lusis, A. J., Snead, M. L. et al. (1993). Genomic structure, chromosomal location, and evolution of the mouse Hox 8 gene. *Genomics* **16**, 123-131.

Bendall, A. J., Ding, J., Hu, G., Shen, M. M. and Abate-Shen, C. (1999). Msx1 antagonizes the myogenic activity of Pax3 in migrating limb muscle precursors. *Development* **126**, 4965-4976.

Carreira, S., Dexter, T. J., Yavuzer, U., Easty, D. J. and Goding, C. R. (1998). Brachyury-related transcription factor Tbx2 and repression of the melanocyte-specific TRP-1 promoter. *Mol. Cell. Biol.* **18**, 5099-5108.

Chalepakis, G. and Gruss, P. (1995). Identification of DNA recognition sequences for the Pax3 paired domain. *Gene* **162**, 267-270.

Chalepakis, G., Goulding, M., Read, A., Strachan, T. and Gruss, P. (1994). Molecular basis of splotch and Waardenburg Pax-3 mutations. *Proc. Natl. Acad. Sci. USA* **91**, 3685-3689.

Conway, S. J., Godt, R. E., Hatcher, C. J., Leatherbury, L., Zolotouchnikov, V. V., Brotto, M. A., Copp, A. J., Kirby, M. L. and Creazzo, T. L. (1997a). Neural crest is involved in development of abnormal myocardial function. *J. Mol. Cell. Cardiol.* **29**, 2675-2685.

Conway, S. J., Henderson, D. J. and Copp, A. J. (1997b). Pax3 is required for cardiac neural crest migration in the mouse: evidence from the splotch (Sp2H) mutant. *Development* **124**, 505-514.

Conway, S. J., Henderson, D. J., Kirby, M. L., Anderson, R. H. and Copp, A. J. (1997c). Development of a lethal congenital heart defect in the splotch (Pax3) mutant mouse. *Cardiovasc. Res.* **36**, 163-173.

Conway, S. J., Bundy, J., Chen, J., Dickman, E., Rogers, R. and Will, B. M. (2000). Decreased neural crest stem cell expansion is responsible for the conotruncal heart defects within the splotch (Sp(2H))/Pax3 mouse mutant. *Cardiovasc. Res.* **47**, 314-328.

Copp, A. J. (1994). Genetic models of mammalian neural tube defects. *Ciba Found. Symp.* **181**, 118-134.

Creazzo, T. L., Godt, R. E., Leatherbury, L., Conway, S. J. and Kirby, M. L. (1998). Role of cardiac neural crest cells in cardiovascular development. *Annu. Rev. Physiol.* **60**, 267-286.

Davidson, D. (1995). The function and evolution of Msx genes: pointers and paradoxes. *Trends Genet.* **11**, 405-411.

Dicke, M. M. (1964). New splotch alleles in the mouse. *J. Heredity* **55**, 97-101.

Eberhard, D., Jimenez, G., Heavey, B. and Busslinger, M. (2000). Transcriptional repression by Pax5 (BSAP) through interaction with corepressors of the Groucho family. *EMBO J.* **19**, 2292-2303.

Edery, P., Lyonnet, S., Mulligan, L. M., Pelet, A., Dow, E., Abel, L., Holder, S., Nihoul-Fekete, C., Ponder, B. A. and Munnich, A. (1994). Mutations of the RET proto-oncogene in Hirschsprung's disease. *Nature* **367**, 378-380.

Epstein, D. J., Vogan, K. J., Trasler, D. G. and Gros, P. (1993). A mutation within intron 3 of the Pax-3 gene produces aberrantly spliced mRNA transcripts in the splotch (Sp) mouse mutant. *Proc. Natl. Acad. Sci. USA* **90**, 532-653.

Epstein, J. A., Lam, P., Jepeal, L., Maas, R. L. and Shapiro, D. N. (1995). Pax3 inhibits myogenic differentiation of cultured myoblast cells. *J. Biol. Chem.* **270**, 11719-11722.

Epstein, J. A., Shapiro, D. N., Cheng, J., Lam, P. Y. and Maas, R. L. (1996). Pax3 modulates expression of the c-Met receptor during limb muscle development. *Proc. Natl. Acad. Sci. USA* **93**, 4213-4218.

Epstein, J. A., Li, J., Lang, D., Chen, F., Brown, C. B., Jin, F., Lu, M. M., Thomas, M., Liu, E., Wessels, A. et al. (2000). Migration of cardiac neural crest cells in Splotch embryos. *Development* **127**, 1869-1878.

Franz, T. (1989). Persistent truncus arteriosus in the Splotch mutant mouse. *Anat. Embryol.* **180**, 457-464.

Galibert, M. D., Yavuzer, U., Dexter, T. J. and Goding, C. R. (1999). Pax3 and regulation of the melanocyte-specific tyrosinase-related protein-1 promoter. *J. Biol. Chem.* **274**, 26894-26900.

Goulding, M. D., Chalepakis, G., Deutsch, U., Erselius, J. R. and Gruss, P. (1991). Pax-3, a novel murine DNA binding protein expressed during early neurogenesis. *EMBO J.* **10**, 1135-1147.

Goulding, M., Sterrer, S., Fleming, J., Balling, R., Nadeau, J., Moore, K. J., Brown, S. D., Steel, K. P. and Gruss, P. (1993). Analysis of the Pax-3 gene in the mouse mutant splotch. *Genomics* **17**, 355-363.

Graham, A., Francis-West, P., Brickell, P. and Lumsden, A. (1994). The signalling molecule BMP4 mediates apoptosis in the rhombencephalic neural crest. *Nature* **372**, 684-686.

Gruss, P. and Walther, C. (1992). Pax in development. *Cell* **69**, 719-722.

Henderson, D. J., Ybot-Gonzalez, P. and Copp, A. J. (1997). Over-expression of the chondroitin sulphate proteoglycan versican is associated with defective neural crest migration in the Pax3 mutant mouse (splotch). *Mech. Dev.* **69**, 39-51.

Hogan, B. (1994). Manipulating the mouse embryo: a laboratory manual. Plainview, NY: Cold Spring Harbor Laboratory Press.

Holland, P. W. (1991). Cloning and evolutionary analysis of msh-like homeobox genes from mouse, zebrafish and ascidian. *Gene* **98**, 253-257.

Hollenbach, A. D., Sublett, J. E., McPherson, C. J. and Grosveld, G. (1999). The Pax3-FKHR oncoprotein is unresponsive to the Pax3-associated repressor hDaxx. *EMBO J.* **18**, 3702-3711.

Jiang, X., Rowitch, D. H., Soriano, P., McMahon, A. P. and Sucov, H. M. (2000). Fate of the mammalian cardiac neural crest. *Development* **127**, 1607-1616.

Kothary, R., Clapoff, S., Darling, S., Perry, M. D., Moran, L. A. and Rossant, J. (1989). Inducible expression of an hsp68-lacZ hybrid gene in transgenic mice. *Development* **105**, 707-714.

Lang, D., Chen, F., Milewski, R., Li, J., Lu, M. M. and Epstein, J. A. (2000). Pax3 is required for enteric ganglia formation and functions with sox10 to modulate expression of c-ret. *J. Clin. Invest.* **106**, 963-971.

Lazik, A. (1999). A role for transcription factor Msx2 in vivo in cardiac neural crest cell development: Msx2 acts downstream of Pax3 to regulate the development of the truncus arteriosus. Ph. D. Thesis, University of Southern California.

Lazik, A., Liu, Y., Bringas, P., Sangiorgi, F. and Maxson, R. (1996). A sensitive method for analyzing beta-galactosidase reporter gene expression in tissue sections of mouse embryos. *Trends Genet.* **12**, 445-447.

Li, J., Liu, K. C., Jin, F., Lu, M. M. and Epstein, J. A. (1999). Transgenic rescue of congenital heart disease and spina bifida in Splotch mice. *Development* **126**, 2495-2503.

Liu, Y. H., Ma, L., Wu, L. Y., Luo, W., Kundu, R., Sangiorgi, F., Snead, M. L. and Maxson, R. (1994). Regulation of the Msx2 homeobox gene during mouse embryogenesis: a transgene with 439 bp of 5′ flanking sequence is expressed exclusively in the apical ectodermal ridge of the developing limb. *Mech. Dev.* **48**, 187-197.

Liu, Y. H., Tang, Z., Kundu, R. K., Wu, L., Luo, W., Zhu, D., Sangiorgi, F., Snead, M. L. and Maxson, R. E. (1999). Msx2 gene dosage influences the number of proliferative osteogenic cells in growth centers of the developing murine skull: a possible mechanism for MSX2-mediated craniosynostosis in humans. *Dev. Biol.* **205**, 260-274.

Louis, T. A. (1981). Confidence intervals for a binomial parameter after observing no successes. *The American Statistician* **35**, 154.

Machado, A. F., Martin, L. J. and Collins, M. D. (2001). Pax3 and the splotch mutations: structure, function, and relationship to teratogenesis, including gene-chemical interactions. *Curr. Pharm. Design* **7**, 751-785.

Mansouri, A., Pla, P., Larue, L. and Gruss, P. (2001). Pax3 acts cell autonomously in the neural tube and somites by controlling cell surface properties. *Development* **128**, 1995-2005.

Manzanares, M., Trainor, P. A., Ariza-McNaughton, L., Nonchev, S. and Krumlauf, R. (2000). Dorsal patterning defects in the hindbrain, roof plate and skeleton in the dreher (dr(J)) mouse mutant. *Mech. Dev.* **94**, 147-156.

Mathieu, M., Bourges, E., Caron, F. and Piussan, C. (1990). Waardenburg's syndrome and severe cyanotic cardiopathy. *Arch. Fr. Pediatr.* **47**, 657-659.

Miyagawa-Tomita, S., Waldo, K., Tomita, H. and Kirby, M. L. (1991). Temporospatial study of the migration and distribution of cardiac neural crest in quail-chick chimeras. *Am. J. Anat.* **192**, 79-88.

Moase, C. E. and Trasler, D. G. (1990). Delayed neural crest cell emigration from Sp and Spd mouse neural tube explants. *Teratology* **42**, 171-182.

Romeo, G., Ronchetto, P., Luo, Y., Barone, V., Seri, M., Ceccherini, I., Pasini, B., Bocciardi, R., Lerone, M., Kaariainen, H. et al. (1994). Point mutations affecting the tyrosine kinase domain of the RET proto- oncogene in Hirschsprung's disease. *Nature* **367**, 377-378.

Satokata, I. and Maas, R. (1994). Msx1 deficient mice exhibit cleft palate and abnormalities of craniofacial and tooth development. *Nat. Genet.* **6**, 348-356.

Satokata, I., Ma, L., Ohshima, H., Bei, M., Woo, I., Nishizawa, K., Maeda, T., Takano, Y., Uchiyama, M., Heaney, S. et al. (2000). Msx2 deficiency in mice causes pleiotropic defects in bone growth and ectodermal organ formation. *Nat. Genet.* **24**, 391-395.

Serbedzija, G. N. and McMahon, A. P. (1997). Analysis of neural crest cell migration in Splotch mice using a neural crest-specific LacZ reporter. *Dev. Biol.* **185**, 139-147.

Shimeld, S. M., McKay, I. J. and Sharpe, P. T. (1996). The murine homeobox gene Msx-3 shows highly restricted expression in the developing neural tube. *Mech. Dev.* **55**, 201-210.

Stuart, E. T., Kioussi, C. and Gruss, P. (1994). Mammalian Pax genes. *Annu. Rev. Genet.* **28**, 219-236.

Takahashi, K., Nuckolls, G. H., Tanaka, O., Semba, I., Takahashi, I., Dashner, R., Shum, L. and Slavkin, H. C. (1998). Adenovirus-mediated ectopic expression of Msx2 in even-numbered rhombomeres induces apoptotic elimination of cranial neural crest cells in ovo. *Development* **125**, 1627-1635.

Tassabehji, M., Newton, V. E. and Read, A. P. (1994). Waardenburg syndrome type 2 caused by mutations in the human microphthalmia (MITF) gene. *Nat. Genet.* **8**, 251-255.

Walther, C. and Gruss, P. (1991). Pax-6, a murine paired box gene, is expressed in the developing CNS. *Development* **113**, 1435-1449.

Wang, W., Chen, X., Xu, H. and Lufkin, T. (1996). Msx3: a novel murine homologue of the Drosophila msh homeobox gene restricted to the dorsal embryonic central nervous system. *Mech. Dev.* **58**, 203-215.

Watanabe, A., Takeda, K., Ploplis, B. and Tachibana, M. (1998). Epistatic relationship between Waardenburg syndrome genes MITF and PAX3. *Nat. Genet.* **18**, 283-286.

Weinstein, D. C. and Hemmati-Brivanlou, A. (1999). Neural induction. *Annu. Rev. Cell Dev. Biol.* **15**, 411-433.